HU ISSN 1785-6892

DESIGN OF MACHINES AND STRUCTURES

A Publication of the University of Miskolc

Volume 3, Number 1 (2013)

Miskolc University Press
2013

HU ISSN 1785-6892

DESIGN OF MACHINES AND STRUCTURES

A Publication of the University of Miskolc

Volume 3, Number 1 (2013)

Miskolc University Press
2013

EDITORIAL BORD

CONTENTS

Design of Machines and Structures, Vol 3, No. 1 (2013) pp. 5–17.

MODELING NONCIRCULAR GEARS WITH COGAL SOFTWARE

ANDRÁS BENDEFY
Budapest University of Technology and Economics
ATTILA PIROS
Budapest University of Technology and Economics

Abstract: Nonlinear racks, noncircular gears and chain rings are special and rare machine parts. The rarity can be explained by the complicated evaluation process of these gears. This introduced project, a numerical method were determined and applied in a computer program, which makes this process easier and faster. The main concepts of the numerical method and the functionality of our software will be shortly presented through some special examples.

Keywords: gear, cogwheel, noncircular gear, nonlinear rack, cog profile.

Introduction

In most cases, general gears defined by basic parameter (module, cog count etc.) are manufactured by special machines [1, 2]. The complicated surfaces of the gears are automatically generated, thus no accurate model is needed. Gear modelling software modules integrated in CAD systems do not reproduce the accurate geometry, as they do not follow the principle of the shear cutting (see Figure 1). These modules serve mostly just to visualize the gears.

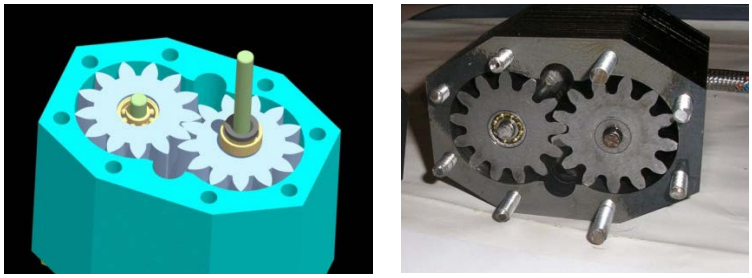

Figure 1. The illustration of gear pump CAD model and the manufactured gear

Recently various CNC technologies came to the front, which are suitable also to manufacture gears, like cutting with laser or water, wire-spark cutting, CNC milling, 3D printing [5]. Contrary to the traditional manufacturing methods, these modern technologies need a precise geometry of the cogwheel. Creating these geometric models of the noncircular gears is usually a slow and difficult process. These machine parts are very rare in the industrial usage, which does not mean that there is no need for them. In many cases, complex mechanisms can be replaced by a single pair of noncircular gear. The reason they are rare, is that their definition is complex and time consuming.

Our main goal was to create a fast and user-friendly software, which can generate a large variety of gear geometry, based on the simulation the rolling of the gears. The method is worked out to calculate noncircular gears, noncircular chain-rings or nonlinear racks (Figure 2 [7]) based on the function of transmission.

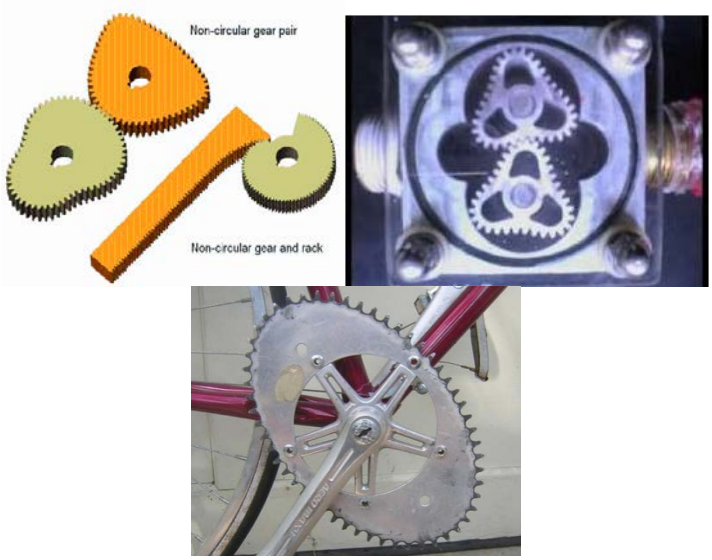

Figure 2. Non-circular gears, non-circular chain-ring and non-linear rack

A non-circular gear can be build up as follows. First, the cog profile must be defined, and then a circular tool-gear must be evaluated. This can be used to generate the non-circular gear after the main curve is defined based on the function of transmission. In the next sections, these methods are presented in details.

1.1. Rolling a line on a convex curve

The circular tool-gear can be generated by rolling a line (the rack) on a circle. Its generalized method is presented here. A steady x–y and a rolling ξ–η coordinate systems are defined. The f_p convex rolling curve is given in the x–y system. The rolling line is defined by the ξ axis on which the predefined f_q cog profiles placed.

$$\begin{bmatrix} X \\ Y \\ (Z) \end{bmatrix} = \begin{bmatrix} X_p(p) \\ Y_p(p) \\ 1 \end{bmatrix} = f_p(p) \qquad (1.1)$$

X = Xp(p); Y = Yp(p)

$$\zeta = \zeta_q;\ \eta = \eta_q(q) + x_{pr} \qquad \begin{bmatrix} \xi \\ \eta \\ (\zeta) \end{bmatrix} = \begin{bmatrix} \xi_q(q) \\ \eta_q(q) + x_{pr} \\ 1 \end{bmatrix} = f_q(q) \tag{1.2}$$

In the (1.1), (1.2) equations the p and q are independent parameters, x_{pr} is the profile displacement.

The rolling is implemented by using finite numbers of transformations of the ξ–η coordinate system. The transformation can be divided into three steps (Figure 3):

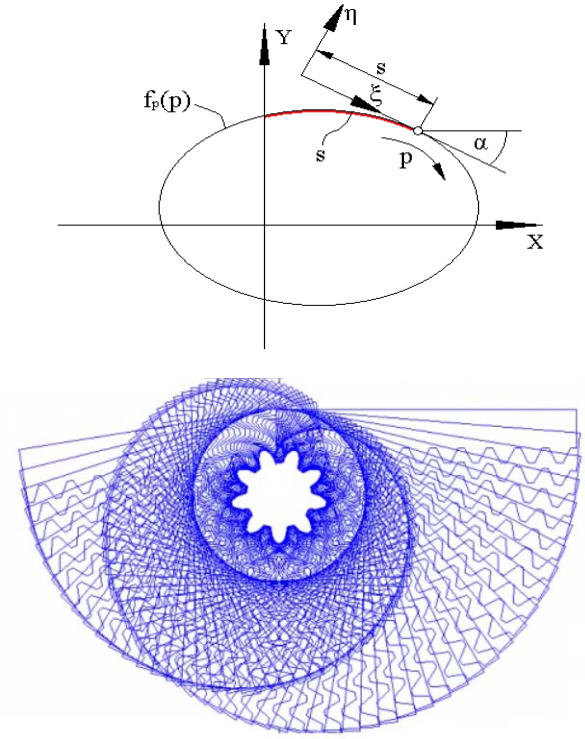

Figure 3. The steps of the transformation and the resultant set of lines

- Offset in the direction of axis ξ with $(-s)$, where s is the rolled length.
- Rotation with α around the centre of ξ–η, where α is the angle of the tangent in the current point.
- Offset of the centre of ξ–η into the current point.

$$s(p) = \int \sqrt{\left(\frac{\partial X_p(p)}{\partial p}\right)^2 \left(\frac{\partial Y_p(p)}{\partial p}\right)^2}\, dp = \int_0^p \sqrt{\left|\frac{\partial f_p(l)}{\partial l}\right|} dl \tag{1.3}$$

$$\alpha(p) = \frac{\arctan\left(\dfrac{\partial Y_p(p)}{\partial p}\right)}{\dfrac{\partial X_p(p)}{\partial p}}. \tag{1.6}$$

These operations are achieved by the following expression.

$$E = T_{xy}\left(T_\alpha\left(T_s f_q(q)\right)\right) =$$

$$= \begin{bmatrix} 1 & 0 & X_p(p) \\ 0 & 1 & Y_p(p) \\ 0 & 0 & 1 \end{bmatrix} \left(\begin{bmatrix} \cos(\alpha(p)) & \sin(\alpha(p)) & 0 \\ -\sin(\alpha(p)) & \cos(\alpha(p)) & 0 \\ 0 & 0 & 1 \end{bmatrix} \left(\begin{bmatrix} 1 & 0 & -s(p) \\ 0 & 1 & 0 \\ 0 & 0 & 1 \end{bmatrix} \begin{bmatrix} \xi_q(q) \\ \eta_q(q) + \chi_{pr} \\ 1 \end{bmatrix} \right) \right) \tag{1.7}$$

For the numeric solution the p and q parameters are not continuous. The f_p and f_q represent the curves not as a function, but as an array of point coordinates.

The result of the transformations is a set of lines (Figure 3). The inside contour gives the geometry of the gear. The details of the contour finding algorithm are presented later [6].

1.2. Rolling a circle on an curve

The determined tool-gear can be used to generate *concave* gears as well. The radius of this circle cannot be larger than the smallest *concave* radius of the f_p rolling curve. The concept of the previous section are used, however, the transformation of the ξ–η system consist of two main steps (Figure 4):

- Rotation with ($\varphi = \alpha + \phi$) around the centre of ξ–η, where α is the angle of the tangent in the current point and $\varphi(p) = s(p)/r$ is the angle of the rolling rotation of the tool-gear.
- Offset of the centre of ξ–η into an offset P_m point.

$$P_m = \begin{bmatrix} X_p(p) + (r + x_p) \cdot \sin(\alpha(p)) \\ Y_p(p) + (r + x_p) \cdot \cos(\alpha(p)) \end{bmatrix} \tag{1.8}$$

r is the radius of the rolling circle in ξ–η.

$$E = T_{mxy}(T_{\alpha\varphi} f_q(q) =$$

$$= \begin{bmatrix} 1 & 0 & mX_{p(p)} \\ 0 & 1 & mY_p(p) \\ 0 & 0 & 1 \end{bmatrix} \left(\begin{bmatrix} \cos(\alpha(p) + \varphi(p)) & \sin(\alpha(p) + \varphi(p)) & 0 \\ -\sin(\alpha(p) + \varphi(p)) & \cos(\alpha(p) + \varphi(p)) & 0 \\ 0 & 0 & 1 \end{bmatrix} \begin{bmatrix} \xi_q)q) \\ \eta_q(q) \\ 1 \end{bmatrix} \right) \tag{1.9}$$

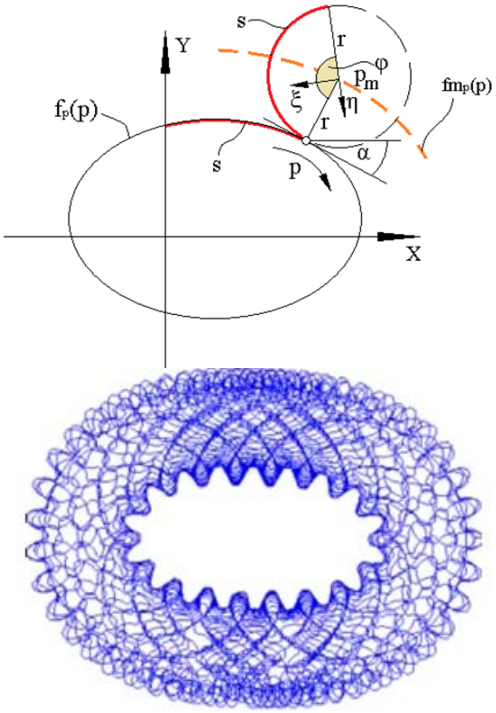

Figure 4. Steps of the rolling of the tool-gear on the rolling curve and the resultant set of lines

With these two methods we can place general cog-profile even on concave rolling curves. The generation of the rolling curves for a given function of transmission is presented in the next section [6].

1.3. Rolling curves

The rolling curves of a pair of noncircular gears which have fixed axis distance can be defined by the *a* axis distance, which is the sum of the working radii $a = r_1 + r_2$ and function of transmission, which is given by

$$i = \frac{\omega_1}{\omega_2} = \frac{\partial\varphi_1}{\partial\varphi_2}, \tag{1.10}$$

where ω_i is the angular velocity, φ_i is the angle position of the i^{th} gears. In Figure 5. Figure 6. a) kinematic chain of the rolling of two non-circular gears is presented. The contact point is placed between the axes. The gears have the same velocity vector in this point, so:

$$r_1\omega_1 = r_2\omega_2. \tag{1.11}$$

Hence, the transmission can be defined by the working radii and/or the axis distance:

$$i = \frac{\omega_1}{\omega_2} = \frac{r_2}{r_1} = \frac{a - r_1}{r_1}. \tag{1.12}$$

Rearranging Eq (4.3), the first rolling curve in polar coordinate system can be define as

$$r_1(\varphi_1) = \frac{a}{i(\varphi_1) + 1} \tag{1.13}$$

and the rolling curve of the second gear can be defined as

$$r_2(\varphi_2(\varphi_1)) = r_1(\varphi_1) i(\varphi_1). \tag{1.14}$$

a)

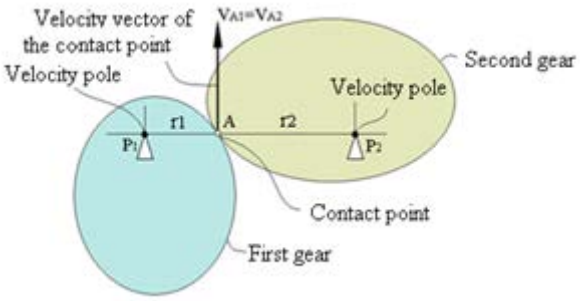

b)

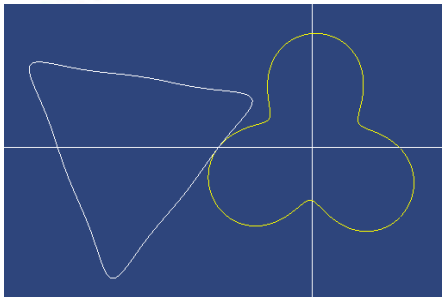

Figure 5. a) Sketch for the evaluation of the curves b) apairs of rolling curves

1.4. Standard cog profile

The analytic definition of the standard cog profile is a quite complicated issue. It contains six different curves with different equations (4 lines and 2 arcs) (Figure 6–7).

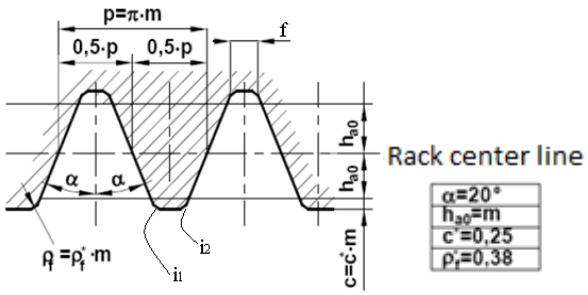

Figure 6. The standard tool rack of a circular cogwheel [5][8]

It is much easier to define just one single period of the profile and then with an algorithm we can make a pattern of it.

Each line entity is defined by two points. The arcs of the profile shape can also be defined by points with a given resolution, so it will contain more short lines.

$$M_p\begin{bmatrix} 0 & f & i_{1x}i_{2x} \\ h_{ao}+C & ha_o+C & i_{1y}i_{2y} \end{bmatrix}. \tag{1.15}$$

The $\mathbf{i}_{1x}$, $\mathbf{i}_{1y}$, $\mathbf{i}_{2x}$ and $\mathbf{i}_{2y}$ vectors have *n* (resolution) elements. These elements are produced by the **q** vector, which also have *n* elements. These elements are changing from 0 to 1 uniformly.

$$q = [q(1)\ \ q(2)\ \ ...q(i)...\ \ q(n)] \tag{1.16}$$

$$q(i) = \frac{i}{n} \tag{1.17}$$

$$i_{x1} = [i_{x1}(1)\ \ i_{x1}(2)\ \ ...i_{x1}(i)...\ \ i_{x1}(n)] \tag{1.18}$$

The arcs (Figure 7) are defined by the (5.5–8) equations.

$$i_{1x}(i) = \rho_f \cdot \cos\left(\left(\frac{\pi}{2}-\alpha\right)\cdot q(i) - \pi + \alpha\right) + \frac{P}{2} + l \tag{1.19}$$

$$i_{1y}(i) = \rho_f \cdot \sin\left(\left(\frac{\pi}{2}-\alpha\right)\cdot q(i) - \pi + \alpha\right) - ha_o - C + \rho \tag{1.20}$$

$$i_{2x}(i) = \rho_f \cdot \cos\left(\left(\frac{\pi}{2}-\alpha\right)\cdot q(i) - \frac{\pi}{2}\right) + \frac{P}{2} + f - l \tag{1.21}$$

$$i_{2y}(i) = \rho_f \cdot \sin\left(\left(\frac{\pi}{2} - \alpha\right) \cdot q(i) - \frac{\pi}{2}\right) - ha_o - C + \rho \tag{1.22}$$

$$f = \frac{P}{2} - 2 \cdot (ha_o + C) \cdot \tan(\alpha) \tag{1.23}$$

$$l = \rho \cdot \tan(\beta) \tag{1.24}$$

$$\beta = \frac{\frac{\pi}{2} - \alpha}{2} \tag{1.25}$$

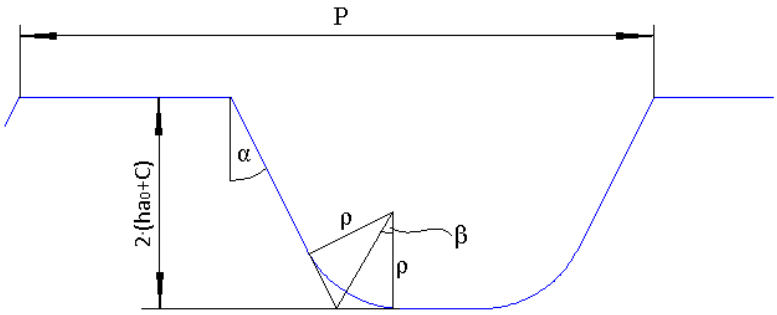

Figure 7. The sketch of the profile, used for the calculation

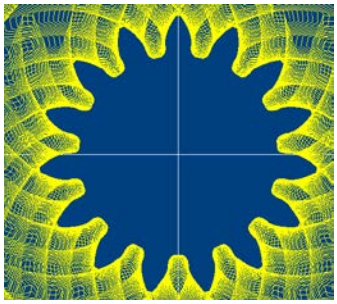

Figure 8. The standard profile rolled on a circle

1.5. Envelope finding

Based on the previous sections, a set of lines can be defined for a general concave non-linear gear (Figure 8). To get the final geometry, we need to find the inside envelope of these lines. Many methods have been developed, implemented and tested, and finally an image based method shows the best and fastest results [4]. The essence of this method is to draw every high resolution raster image of the lines using the graphics card. From this image we can obtain the contour, pixel by pixel very rapidly by using the GPU (Figure 9).

Some filtering methods are also applied on the final geometry. The resolution of the applied image can be adjusted to the given surface tolerance of the gear surface.

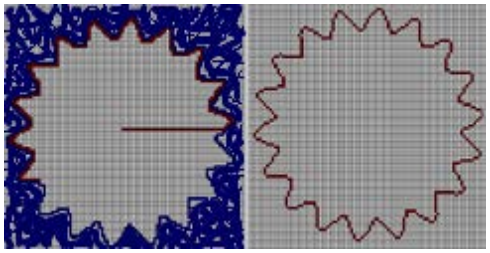

Figure 9. Image based contour finding presented in a very low resolution

1.6. The cogal application

For ease of the more convenient use, the previously reviewed computations were implemented in C# environment. The name of the software: CogAL, derived from "***Co***gwheel ***g***enerator ***al***gorithm". Our goal was to create an easy-to-use application for circular and non-circular gears and non-linear racks (Figure 10). In the next subsections, the four separate functions of the program will be covered.

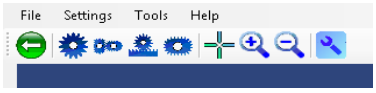

Figure 10. The menubar of the main functions

Generating a circular gear

This module can generate circular gears with multiple types of profiles. The standard profile can be defined with its main parameters (like module, contact angle etc.) (Figure 11). Aside from the standard trapezoid profile, it is possible to define sine, chain and custom profiles.

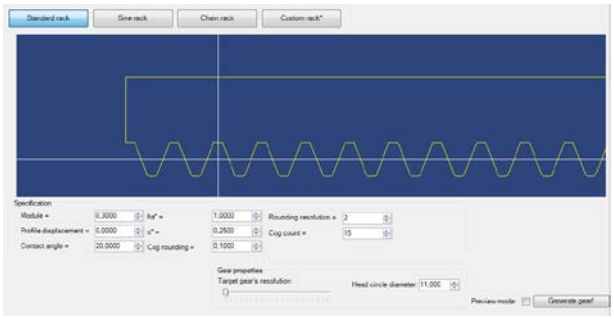

Figure 11. CogAl's circular gear generator module

Generating non-circular gear pair, with fixed axis distance

To generate this kind of gear pairs, three steps have to be taken. The first step is to define the rolling curves with their axis distance, and the angle positions pairs (see Figure 10 a). The angle positions can be defined by a function or by a CSV table.
In the next step, the profile has to be specified similarly to the *circular gear* section. When both the profile and the lines are available, a preview image of the final geometry will be generated (Figure 10 b).

In the final step the program will find the contour of the preview shape. The final geometry will be generated. This geometry is available for further usage, like exporting into standard CAD system format or a real-time rolling test of the final gears geometries can be performed to check the result (Figure 11).

a)

b)

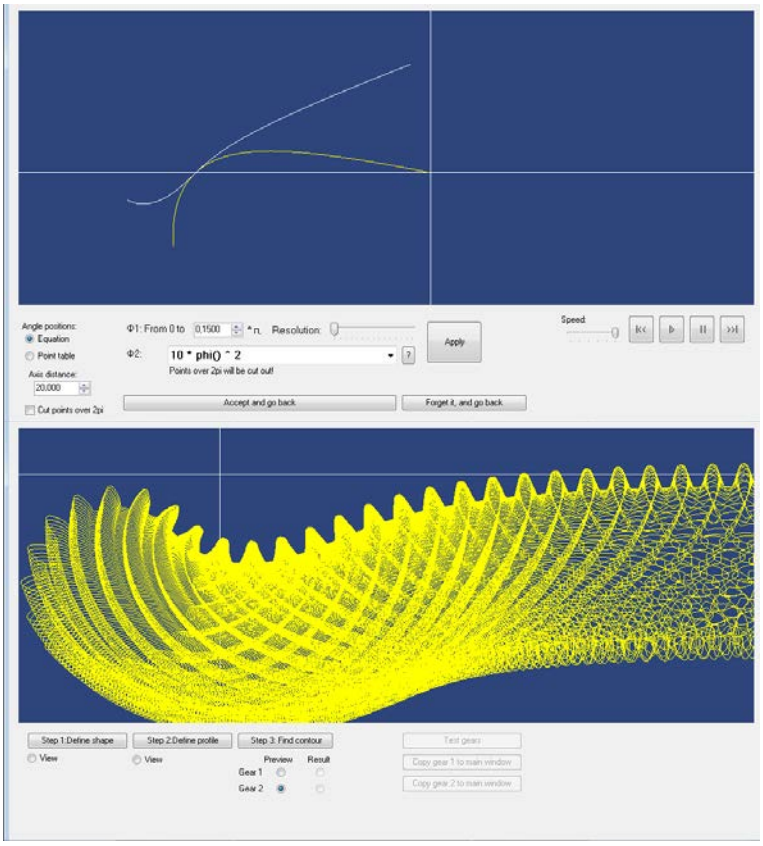

Figure 12. a) Generated the rolling curves in CogAl b) Preview of the final geometry

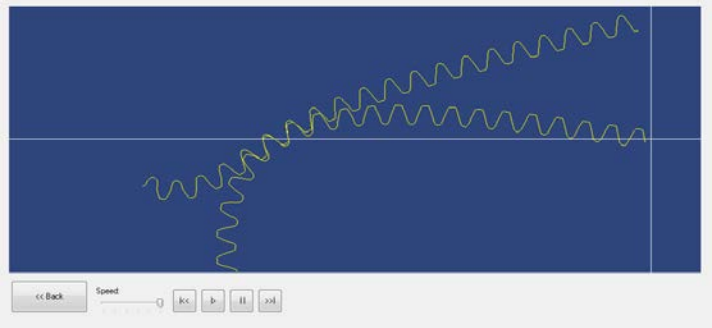

Figure 13. CogAl shows the final geometry of the non-circular gear pair

Generating non-circular gear-rack pair

The use of this module is similar in many aspects to the previously presented module. The main difference is in the first step, where the position of the rack is specified as a function of the angular position of the cog-wheel. In this case the transmission function has length units and there is no need to give an axis distance (as it theoretically would be infinite in each case) (Figure 14).

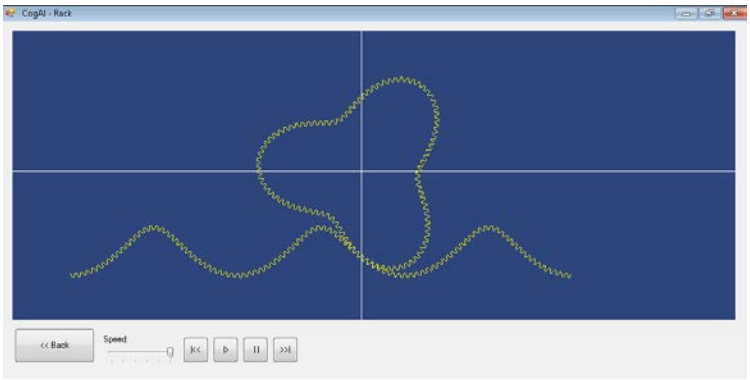

Figure 14. CogAl shows the final geometry of the non-linear gear-rack pair

Generating a single, non-circular gear with arbitrary rolling curve

This module can generate a non-circular gear with any kind of rolling curve, with standard, sine, chain or custom tooth profiles. The rolling curve can be defined with two parametric functions in Cartesian or polar coordinate systems, or by loading a CSV file that contains the coordinates (Figure 15).

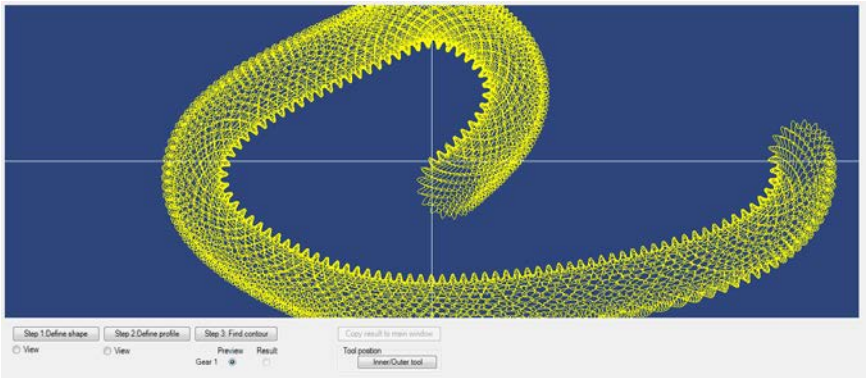

Figure15. Generating a single gear with arbitrary curve by CogAl, using the curve of the gears shape

1.7. Examples

In this section some test applications are shown where the capability of the software and the validity of the results are shown.

In the first test, two gears with identical rolling curves were generated, which creates periodical pulsation in the transmission function. The functions of the angular positions were determined by sinusoidal functions [Figure 14 a)].

The second example shows a non-circular gear pair which compensates the angular velocity pulsation of a 45° cardan joint [Figure 14 b)].

In the next model we balanced a weight on the end of an arm, using a spring and special rack. The weights torque changes in the axis as we move the arm. The special rack and gear connection between the arm and spring equals the loads, so the weight is balanced in every position.

In the least example, a two-bar open kinematic chain is created, where the linear motion of the end point is guaranteed by non-circular gears, which crates the proper transmission function between angular positions of the bars [Figure 14 d)].

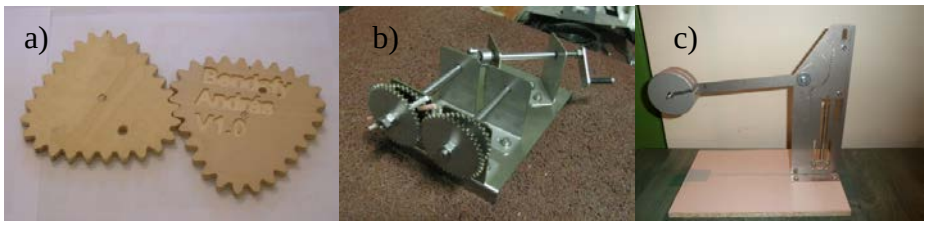

Figure 16. a) Gears for harmonically varying transmission. b) Eliminating the angular velocity pulsation of the cardan joint. c) Balancing a weight with spring and special rack

Figure 17. Open kinematic chain with linear motion of the free end

1.8. CONCLUSION

In this project a software was created which is able to generate general concave non-circular gears, based on a few parameters. The implemented numerical methods were analyzed and optimized to create a fast and reliable geometrical result of the generated cogwheel. A user friendly interface is created where only the main parameters are required and the additional computation is evaluated in the background. The efficiency of the software is represented thorough some engineering examples.

The program is still under development, but it is aimed that later it should be applicable individually, even integrated into CAD system.

1.9. References

1. F. L. Litvin: *A fogaskerékkapcsolódás elmélete.* Műszaki Könyvkiadó, Budapest, 1972.
2. Erney György: *Fogaskerekek.* Műszaki Könyvkiadó, Budapest, 1983.
3. Simon Vilmos: *Gépelemek 2.* Budapesti Műszaki és Gazdaságtudományi Egyetem, 2008.
4. Bach Iván: *Formális nyelvek.* Typotex, Budapest, 2002.
5. Fisher, U.: *Metal tables*. Haan-Gruiten: Verlag Europa-Lehrmittel, 1999.
6. Egerszegi János–Laczik Bálint: *Nem köralakú fogaskerekek a fegyvertechnikában*. Zrínyi Miklós Nemzetvédelmi Egyetem Bolyai János Hadmérnöki Kar.
7. Laczik Bálint: *Cometarium-mechanizmus*. Fizikai szemle, 2008/2.

Design of Machines and Structures, Vol. 3, No. 1 (2013), pp. 19–24.

CHANGE OF TOOTH ROOT STRESS CALCULATION MODEL FOR NON-SYMMETRIC TOOTH SHAPE

ZSUZSA DRÁGÁR–LÁSZLÓ KAMONDI
Department of Machine and Product Design, University of Miskolc
H-3515 Miskolc-Egyetemváros
machdzs@uni-miskolc.hu; machkl@uni-miskolc.hu

Abstract: In gear design the calculation of the strength has great important that national or international standards ordain. Models in these directives apply gears of symmetric tooth shape. In case of gears rotating in one direction asymmetric tooth shape arises. Model should be modified for calculations of non symmetric tooth shape.
Keywords: tooth root stress, non-symmetric teeth.

1. Introduction

In gear design many aspects have to be considered. For the calculation of the strength, the knowledge of the forces acting on the gear teeth, the possible failure forms of the machine elements and the material properties of the gear body are necessary depending on the type of the gear drive [2]. The basic standards for the sizing provide guidance in the gear design with symmetric teeth. Nowadays, the researchers have published several results on the possibility of the formation of asymmetric gears (see e.g., [6]). The need for this kind of change is primarily aimed by increasing the load capacity of the gears. Non-symmetric gear tooth shape can arise for power drives when gears are rotating in the same direction.

In this paper we are dealing with the determination of the stress at the tooth root for non-symmetric tooth shape for strength scaling.

2. Development of the strength scaling

The strength scaling processes has been changing significantly in the past two hundred years. In 1822, Tredgold was the first who introduced the strength calculations in sizing of the gears [2]. The attack of the force has been assumed on the edge of the head. This method has been further developed by Bach applying the idea that the body force was substituted by distributed force along the length of the tooth [1]. However, these calculation methods didn't follow the exact shape of the tooth.

Later, with the expansion of knowledge and experience, the specific gear failures, which are primarily affected by the operating conditions, were also considered. Therefore, the stress at the tooth root, the surface pressure and the seizure were based in the sizing. These calculation principles were separated in time.

The earliest, the scaling for the tooth root capacity was spread. In 1893, Lewis developed a computational method that is taking into consideration the tooth shape [2]. The tooth, which was substituted by a parabola of uniform strength, was handled as a beam clamped at one end, i.e., a cantilever, and the loading force was assumed to be an evenly distributed force along the tooth length. His model is exhibited on Figure 1.

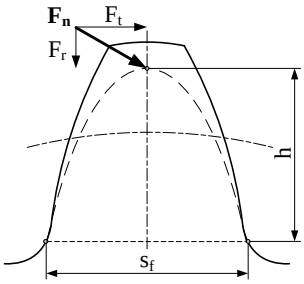

Figure 1. Lewis' model

For bending, the most dangerous section of the tooth is pointed by the point of the parabola which is tangent to the tooth root curve. The introduction of the notion of the tooth form factor is linked to Lewis.

Later Hofer refined Lewis' model. He marked out the dangerous section of the tooth root by straight lines angled 30° with the tooth centre line [3].

In 1908, Vidéky called the attention to the sizing for the surface pressure and through that for the influence of Hertz-stresses [1]. This method was further developed by Buckingham in 1926.

The seizure phenomenon called the researchers' attention to the warm-up conditions [2]. In this topic, Almen and Block got results in 1937. Dudley determined the required lifetime of gears through his calculations in 1954. Niemann developed a method in 1965, how to calculate with the actual operating conditions.

In 1950's, research works were published at both national and international levels on the gear strength scaling [1], [2]. The design recommendations of the American Gear Manufacturers Association (AGMA) have been published. Ten years later, in 1970, the national standard DIN3990 – in West Germany – and the international standard ISO 6336 were issued. Nowadays, the main regulations governing the calculation of the tooth root stress are summarized in ANSI/AGMA 2101-D04 (2004), DIN 3990-3 (1987), ISO 6336-3:2006 (see [5]).

3. Model creation

The models applied in strength calculations for the determination of the load capacity of the tooth are partially different. The difference is mostly due to the fact that which component of the load force on the tooth or normal tooth force is taken into account. The components of the normal tooth force, which is perpendicular to the toot surface, raise different stresses at the tooth root. The tangential component rises bending and shears at the tooth root and the radial component causes pressure on the root [1]. The difference between the calculations is due to the fact that which stress the calculation is performed on. The models contain simplifications of the real operating circumstances which are taken into consideration into the model with various modifying factors. Some of these factors depend on the geometry of the model.

For the calculation of the carrying capacity of the tooth root, one has to determine the nominal stress at the tooth root. The directives contain data of sizing for bending stress. The general form of the applied formula is given by expression (1), where σ_F describes the nominal stress at the tooth root, b denotes tooth width, F_t the tangential component of the

normal tooth force, m the module and Y_F stands for the tooth form factor. The calculation is to be performed on both members of the gear pair.

$$\sigma_F = \frac{F_t}{bm} Y_F \cdot \tag{1}$$

In each system, the determination of the tooth form factor depends on the type of the model. This means that the design methods can not be applied such that the tooth form factor is taken over from another method.

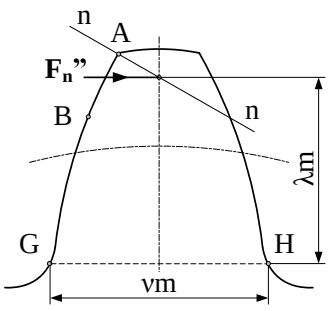

Figure 2. The calculation scheme of the load capacity of the tooth root when the bending is taken into consideration (Model 1)

On Figure 2, n-n denotes the line of action of the normal tooth force. Model 1 assumes that the tangential component of the normal tooth force load the tooth root is purely on bending and the tooth form factor is deduced from the bending stress written for the point G. This can be done when the normal tooth force is acting at an individual point (A) or at dual connection points (B). The values of ν and λ can be determined from the point set P_i (x_i, y_i) (i = 1, 2, …, n) of the base profile obtained by geometric mapping which is described by geometric conditions [8].

Model 2 is shown on Figure 3. The tooth form factor is deduced from the tooth root stress at the point G and it counts with both components of the normal tooth force.

On Figure 4, Model 3 considers the friction phenomenon at the contact points as well. At the entry of the contact, slipping occurs besides rolling (slipping with rolling). The resulting friction force together with the normal tooth force will change the load on the tooth. The tooth root stress, calculated at the point G will provide a different form as in Model 1 or in Model 2.

The calculation method of the tooth form factor should not be transferred from one system to another because the determining factors of the maximum value of the tooth root stress are also depend on the tooth shape and on the model.

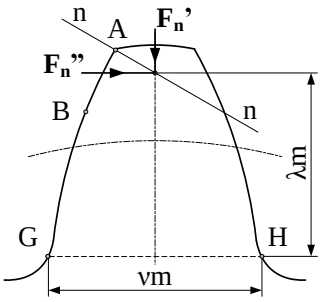

Figure 3. Both the bending and pressure are taken into consideration in the model of the load capacity for the tooth root (Model 2)

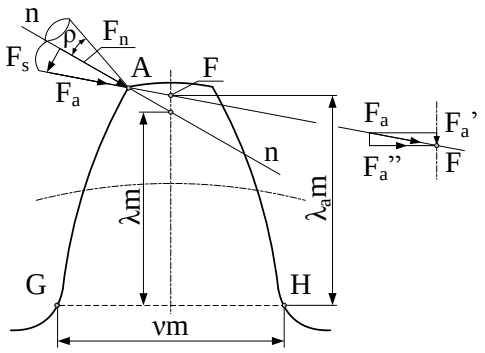

Figure 4. The load capacity model with the phenomena of bending, pressure and friction (Model 3)

4. Deviating from the standard

In case of gears rotating in the same direction, in a number of studies it was proved that the load capacity can be increased by the application of asymmetric toothed gears [7]. Di Francesco and Marini [7] have developed a computational method which allows the sizing of asymmetric gear teeth. Their concept is based on the ISO standard. The simplified view of their model is exhibited on Figure 5.

On the figure, the asymmetric tooth is denoted by letters HCAK'I', the left side of the tooth is the active (load transfer) side. The symmetric tooth is indicated by HCDKI. In the model, the cross section dangerous for bending (line HK') is located at the same distance from the gear centre as the cross section of the symmetric tooth (line HK) dangerous for bending. Line HK is appointed by the tangent lines which have angle 30° with the centre line of the symmetric tooth. Point L' bisects HK'. The axis of the asymmetric tooth passes through the point L'.

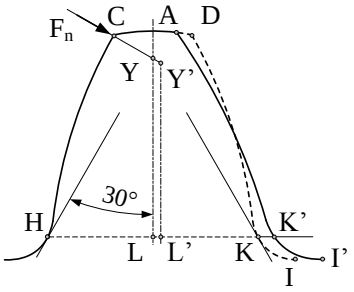

Figure 5. Asymmetric tooth model by Di Francesco and Marini

The point Y' on the axis of the asymmetric tooth is the intersection point of the axis and the line of action of the normal tooth force. The authors took the distance between the dangerous cross section and the force component causing bending at the tooth root with LY due to the small difference.

It should be noted that this approximation is not applicable for each model as the difference between LY and L'Y' is not negligible e.g., at the model which counts with the friction, the intersection point of the line of action of the force and the modified symmetry line can result significantly larger deviation.

Returning back to the model of [7], the authors have taken distance LY as the arm of the bending force. The difference comparing to the symmetrical tooth was resulted by the change of the tooth form factor and the stress concentration factor in the dangerous cross section (HK').

5. Deviating from the standard

If we modify the model then we have to change the tooth form factor at the same time. According to the normal tooth force loading to the tooth and the friction, the asymmetry of the tooth causes significant changes in the model.

The operational and supporting sides of the tooth are different which phenomenon is generated by the different profile angles of the basic profile and the different radii of the top roundings at the tooth root. As a result, the cross section of the tooth root will change, will increase, which is also modified by the number of teeth and the profile shift when we do not use uncorrected toothing.

The concept of the proper choice of the "new" dangerous cross section and the placement of the axis of this section is an important question.

Due to the changed geometry, an additional question arises: where the greatest stress occurs in the tooth root? The tangent line to the tooth root curve for involute derived by profile angle different than 20°, can be edited with another angle to the axis of the asymmetric tooth as in the symmetric case. These questions need to be answered after calculations.

Among the factors involved in the nominal tooth root stress, beside the tooth form factor the stress concentration factor depends on the geometrical shape of the model. This paper is not concerned with the latter.

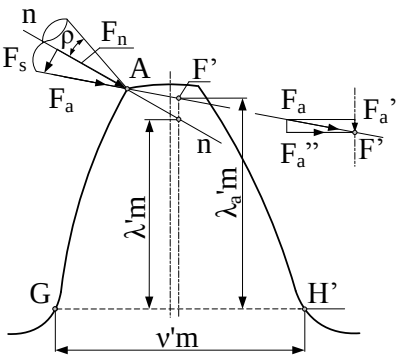

Figure 6. Computational model for asymmetric tooth

6. Summary

The standards of gear sizing are developed for the strength calculation of the symmetric tooth shape for specific model describing the geometry of the tooth. In case of power drives, the sizing is basically done for bearing capacity of the tooth root. A number of researches are published on the applicability of the asymmetric tooth gears from the point of increasing the capacity. Computational models have been proposed for the modifications which handle the asymmetry. In order to approximate the processes more accurately it is necessary to develop model which follows better the changes of the geometry and which takes into consideration the friction besides the components of the normal tooth force.

7. Acknowledgement

The research work presented in this study based on the results achieved within the TÁMOP-4.2.1.B-10/2/KONV-2010-0001 project and carried out as part of the TÁMOP-4.1.1.C-12/1/KONV-2012-0002 „Cooperation between higher education, research institutes and automotive industry" project in the framework of the New Széchenyi Plan. The realization of this project is supported by the Hungarian Government, by the European Union, and co-financed by the European Social Fund.

8. References

[1] Erney Gy.: *Fogaskerekek*. Műszaki Könyvkiadó, Budapest, 1983.
[2] Zsáry Á.: *Gépelemek II. kötet*. Nemzeti Tankönyvkiadó, Budapest, 1990.
[3] Vörös I.: *Fogaskerekek fogalakjai és fogalaktényezői a fogtőszilárdság méretezéséhez*. Akadémiai Kiadó, Budapest, 1968.
[4] DIN3990 Tragfähigkeitsberechnung von Stirnrädern, 1987.
[5] Eurotrans Technical Committee: Equivalence between ISO Standards and National Standards (Concerning Gear Technology) p. 7.
[6] A. Kapelevich: *Geometry and design of involute spur gears with asymmetric teeth*. Mechanism and Machine Theory 35 (2000), pp. 117–130.
[7] G. Di Francesco–S. Marini: *Asymmetric Teeth: Bending Stress Calculation*. Geartechnology, March/April 2007, pp. 52–55.
[8] Kamondi L.–Drágár Zs.: *Asymmetrical teeth meshing near general centre distance*. International Journal Advanced Engineering, 6 (2012) No. 1, pp. 31–42.

Design of Machines and Structures, Vol. 3, No. 1 (2013), pp. 25–32.

CORKSCREW DESIGN

ZOLTÁN TAMÁS KOVÁCS – ÁGNES TAKÁCS
University of Miskolc, Department of Machine and Product Design
3515, Miskolc-Egyetemváros
adatfalo@gmail.com

"This is clear for me science and technology does not solve every problem.
But without science and technology you cannot solve any problem."
Ede Teller

Design is a (kind of) creative activity, the main objective of which is to define the characteristics of the designed machines or products. These characteristics are not just the outside features of the machines but also the fundamental structural and functional parts of them. The quality of the design is determined by several factors like the harmony between the cultural, the technical, the economic and most of all the functional aspects of the design and the flow between the aforementioned categories. The goal of the design is to create a colourful quality of the objects in their whole lifecycle. So the designer is not only responsible for defining the product concept, but also has to pay attention to the mechanical computations, regulations of the law, producability etc.

1. Introduction

Our everyday life is full of difficulties, so we need moments of harmony and tranquillity that can mean a glass of wine with friends, but to do that, we need a good wine and the perfect corkscrew. So the following question is answered: Why the design a corkscrew? This paper tries to give an answer to the question what is the ideal shape and appearance of a corkscrew.

The product design – the art of shapes – creates the connection between the object and the user of the object. At the same time, it defines the usage of the object, so it becomes an integral part of our lives. The quality of these objects reflects the way we perceive our environment.

2. Market Research

The development of different objects, tools, the design development, the process of the change are specific forms of evolution, which are influenced by one's own will. First of all the culture history of the corkscrew will be presented in this chapter than the evolutionary aspect of the shape will be considered. The chapter also presents the common ancestors of the introduced shape from which today's modern corkscrew can be derived.

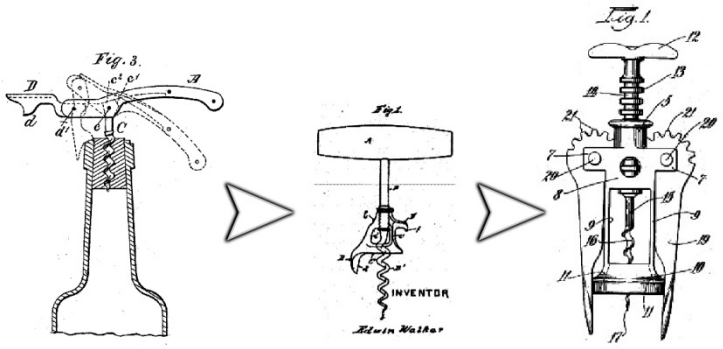

Figure 1. Famous Corkscrew Types (left to right) 'Butler's Friend' by C. Wienke, Walker Bell by E. Walker, Double Winged Lever Corkscrew by D. Rosati

The thesis has striven for uniqueness in the technical and design aspects of the object but also puts great emphasis on the designs be in harmony with nature as well. During the design of the product to the ecological design criteria was also payed attention such as the material selection, the efficiency of materials, energy and the use of technology, reversibility, long life, and upgradability.

Taking the environmental aspects of the design into consideration were the product packaging materials and packaging techniques chosen. Because of the characteristic of the product the ergonomic approach were combined with the experience from the market mainly the hands-on needs were examined and that is why I made different versions of the product.

Type	Weight (kg)	Weight (N)
T-Corkscrew	22 Kg	215–245 N
Single Lever Corkscrews	18 Kg	176–206 N
Double Winged Lever Corkscrew	12 Kg	117–147 N
Temperature at the start of the experiment:	22 °C	
Temperature at the end of the experiment:	22°C	
Moisture at the start of the experiment:	50%	
Moisture at the end of the experiment:	51%	

Figure 2. Data from the experiment

The best circumstances for the design were examined, evaluated and proved with measurements and finite element calculations. Then they were modelled with a 3Dmodeler software and animations were made from the product.

3. Ergonomics

Ergonomics is the study of the interaction between people and machines and the factors that affect the interaction. Its purpose is to improve the performance of systems by improving human machine interaction. This can be done by ‘designing-in’ a better interface or by

'designing-out' factors in the work environment, in the task, or in the organisation of work that degrade human–machine performance.

3.1. Power of the hand

Studies referring to human pressure have shown that the biggest pressure a person can apply to the atlas of the human body is 30 kg/cm^2 at most if the subject is between 20–36 years old, 25 kg/cm^2 if he/she is between 36–50 years old and they can be pressed by 20 kg/cm^2 in the case of the subjects over 50 years old. When taking the research results into consideration. The maximum amount of applicable pressure applied during occasional lifting was determined.

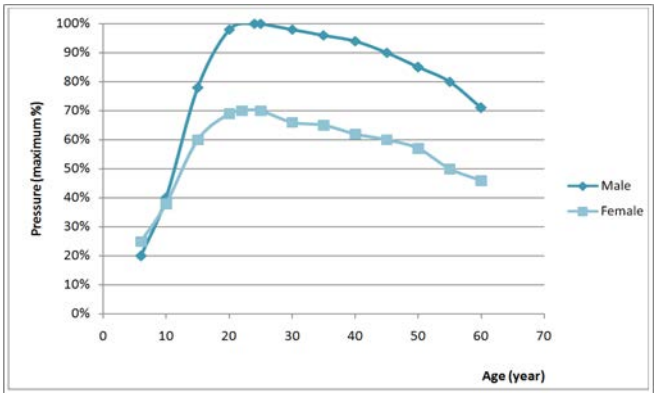

Figure 3. Age and gender effect to maximum applicable pressure

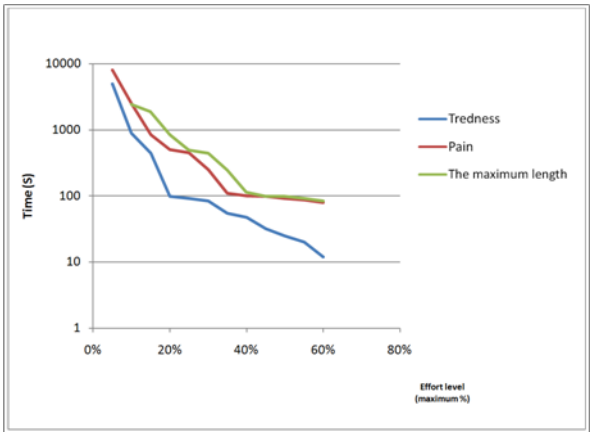

Figure 4. Beginning of tiredness and pain according to the percentage of elbow strength

Physical effort spreads in an optimal way across the surface of one's palm when the grip of the tool used has contact with a great area of the fingers and the cushioned parts of the palm. To achieve this, relatively thick, curved "wings" are required. These wings should have a flat surface, fit the palm and follow the curves of the grasping fingers. The push-and-pull force and the gripping surface area are the most important ergonomic features of a

corkscrew. Between the best and the worst corkscrews the necessary strength hand the surface of fitting fingers and palm scan vary by 100%, which results in only a quarter of the pressure on the palm tops in the best case.

$$degree\ of\ \ fit = \frac{concerned\ \ gripping\ \ surface}{entire\ \ gripping\ \ surface}.$$

The maximum palm force achievable depends greatly on the distance of the corkscrew's wings. Due to different hand sizes, the optimum is about 70 mm for men and 60 mm for women. Shorter and longer distances can significantly decrease the maximum force one can muster. Trendy slim and curved grips are often so close to each other that one's fingers can get stuck in between. Only tools with proper wing distances are worth being designed to avoid it. Also, the two wings grasped in the hands should be thick enough, so that the fingers cannot clench them fully. A full clench can lead to the fingertips and nails constantly be crashed to the palm.

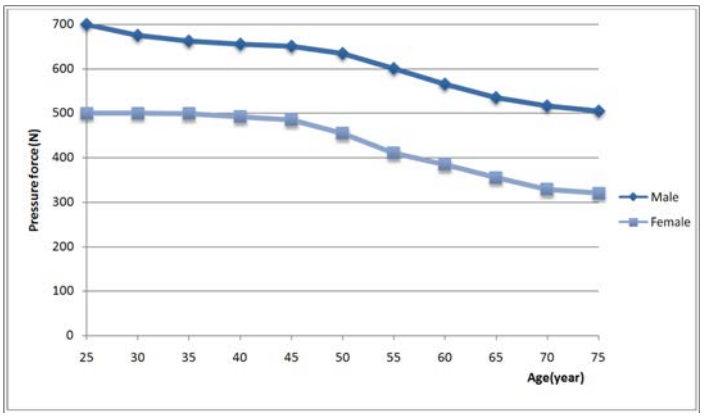

Figure 5. Age factor to the maximum applicable pressure differentiating between genders

3.2. Conclusion

Today the importance and bloom of product ergonomics have several reasons, for example, it is getting more recognition from the economy and this has been created the marketing based design. Furthermore the clamp-down regulations also helped the development of the product ergonomics. Nowadays designers put much more emphasis on satisfying the needs of niche segments like elderly or disabled people. Also ergonomics has become a social norm so more and more people demand it, which leads to more studies on the subject and also more products based on these studies.

4. Eco-design

Waste management and preventing pollution are the basic motives of environmental protection parties but these strategies only mean to minimalize or prevent some kinds of effects but ignoring the design of the object. The eco-friendly design put the process of the

design into the outmost importance of the designer engineer. This way the effects on the environment deriving from the product and the manufacturing process can already be reduced from the birth of the design. Almost 80% of the pollution, which will be created by the product can be determined at the design phase of the production. Concerning the costs of the product life cycle, the situation is the same. This is the reason why it is significant that we calculate with the economic and environmental impact of the product from the beginning.

4.1. Design for the Life Cycle

Most important features of the Kenneth Crow life cycle design:

- Analyzability
- Usability
- Trustworthy
- Reparability
- Eco-friendly design
- Improvability
- Mounting
- Safety and product responsibility
- Ergonomic human characteristics

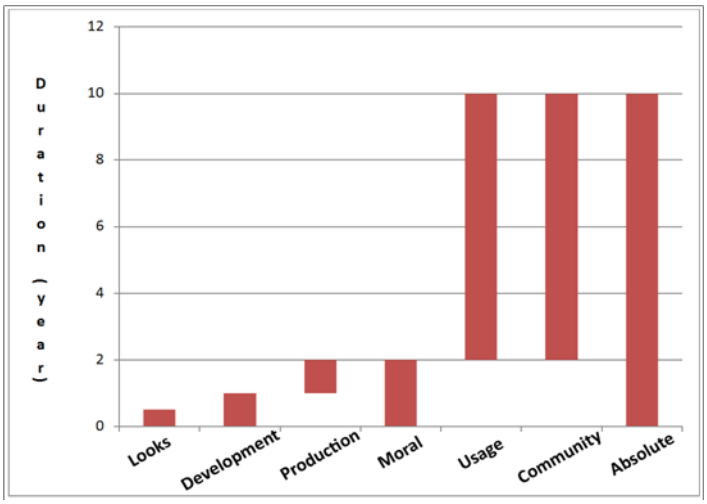

Figure 6. The assumed lifecycle of the screwdriver

5. Concept and design

5.1. Logo as a symbol

When the logo came to be designed, besides the function of the corkscrew the main aspect was its eco-friendly message. The grape leaf positioned above the letters and the wavy line running down to the letters evoke plant ornament but it can also be associated with the corkscrew or the connection of leaves to the grapevine or even the letter “i” in the Latin word “veritas”.

Grapes and a grape leaf have a rich symbol system, Sumerian cuneiform script marked the word life with a sign resembling a grape leaf. It frequently appears in Roman art: its meaning is abundance and joy. This symbolism can be connected to Bacchus (the Roman equivalent of Dionysus). He is the god of vine, sexuality, fertility even pleasure and expressiveness. According to a Jewish tradition, the tree in Eden was a grapevine.

The Bible has Noah, the father of humanity after the flood, as the first man to cultivate grapevines. The name of Deucalion (the “Greek Noah”) literally means “New Wine Sailor”. Grape coming from the Land of Promise meant the possibility of new life for the Jews. Christians believes that wine is the blood of Jesus.

Figure 7. The designed logo

6. Realization

After the researches and calculations done, the most favourite part of the designers' job comes, which is the conceptual design. After the physical and shape requirements had done the double winged lever seemed to be a viable conception. Three 2D sketches were created by which the most viable version was modelled in 3D then textured and rendered as it is shown in Figure 8 to Figure 10.

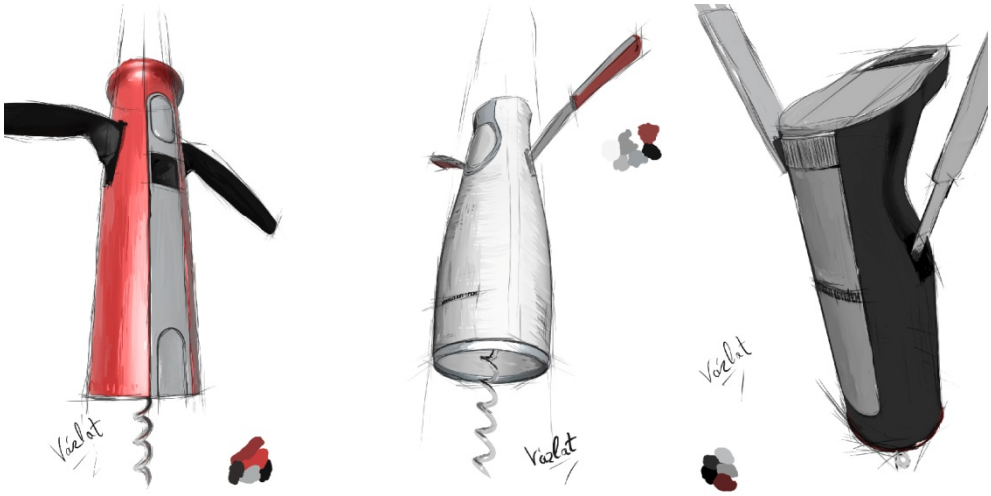

Figure 8. The 2D drafts

Figure 9. Eco-Friendly Pack Concept

Figure 10. The 3D model

Figure 11. The final concept

Acknowledgement

This research was supported by the European Union and the State of Hungary, co-financed by the European Social Fund in the framework of TÁMOP-4.2.4.A/2-11/1-2012-0001 'National Excellence Program'.

References

[1] Bridger, R. S.: *Introduction to Ergonomics*. 1995.
[2] Moser M.–Pálmai Gy.: *A környezetvédelem alapjai*. Felsőoktatási tankönyv, 2006.
[3] Herczegfi K.–Izsó L.: *Ergonómia*. Typotex Kiadó, Budapest, 2010.
[4] Schischke K.–Hagelüken M.–Steffenhagen G.: *Bevezetés az Öko-Design Stratégiáiba – Miért, mit és hogyan?* Berlin, 2005.

Design of Machines and Structures, Vol. 3, No. 1 (2013), pp. 33–38.

VIRTUAL RECONSTRUCTION OF AN ANCIENT PIECE

MELINDA MAJOROS–ESZTER VARGA–ATTILA PIROS
Department of Machine and Product Design
Budapest University of Technology and Economics, Budapest, Hungary
H-1111 Budapest
majorosvarga@gmail.com

Abstract: Our research topic is to present how to remake the original geometry and the visualization of a 16th century piece in CAD system. This article gives an overview, which introduce a complex method we used to create solid body from a scanned point cloud, on which different virtual simulations can be carried out. For the solution of the task we have developed a method for creating a surface texture, which is capable of displaying photo-realistic virtual models as well. The process itself innovative and novel, which can be used in varied places and it can also facilitate the manual restoration procedure.
Keywords: geometry reconstruction, texture mapping, visualization method

1. Introduction

The method we developed is a new and simple reverse engineering technique. The process gives a complex solution to create an accurate CAD model and a perfect visualization from a real object after 3D scanning. The innovation of the method is to combine the remake of these sections in a simple and a realistic manner which haven't been used before in this kind of accuracy. In fact the process is a type of undistorted digitalization technique which more than 3D scanning. The visualization is based on photograph distortions, which also gives a better result than previously used reverse engineering software's color data detection. In the following article the base of the method will introduce. Other automation needed to make the usage of the process suitable for every piece.

2. Recording data

In the beginning of the reconstruction data digitalization was needed. The real object was used as the source of all detected data. We used a 16^{th} century vase to introduce the process. In the beginning a 3D laser scanner scanned the surface of the ancient piece. The inner and the outward faces were scanned in rotary scan type (Figure 1). The density of the points was important in the process to evince all the surface finish. The brightness of the coated areas didn't have effect on the final result of the scanning. Extra points were erased from the point cloud.

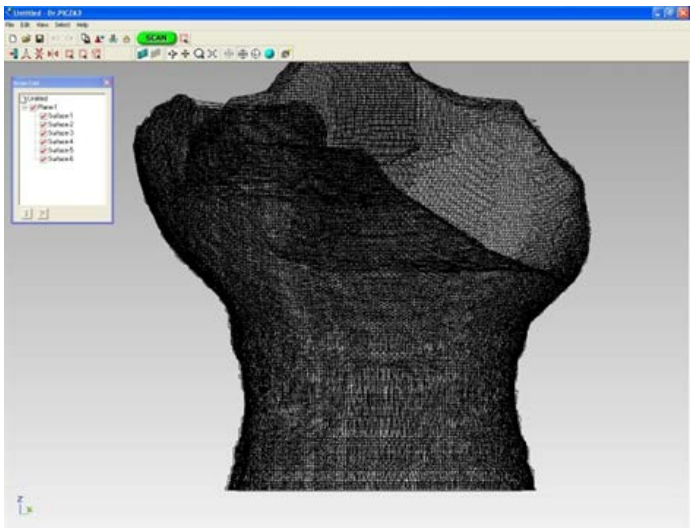

Figure 1. Point cloud of the 3D laser scanning

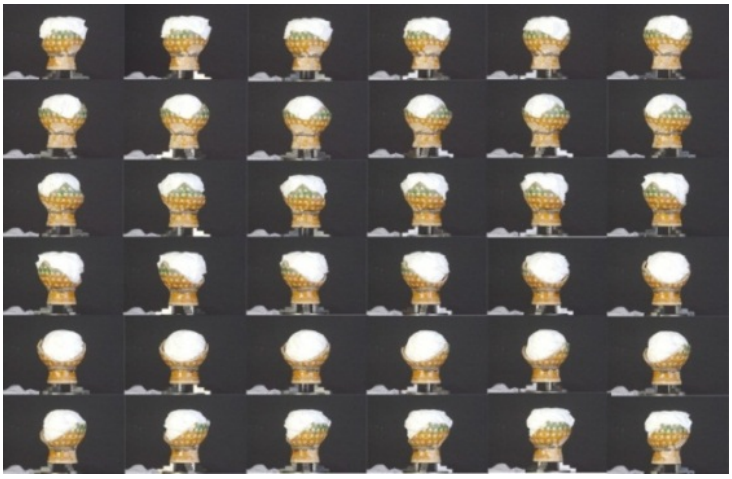

Figure 2. The photographs in studio environment

After the scanning process, photographs were made in studio environment. All the setting of the photographing was previously deliberate and fixed. The vase was placed on a turn table which was suitable for precise rotation. The piece was rotate about the axis and photographs were taken in every 10 degree. The target was to get 36 different photographs from the same view with the same light and environment settings. (Figure 2). After having the adjusted photographs pictures were generated on computer from the digital negatives. Subsequent photo corrections were needed to reconstruct the original colors and directions

in every digital picture. Absolute gray card was the reference of the original colors to minimalize the accidental effects of the camera and the artificial lights.

3. Geometry reconstruction

In a parallel way the reconstruction of the real body of the vase was started in CAD software called PTC Creo. In the first step of manipulation of the point cloud was needed along the borders to remove the extra parts. Afterwards cylindrical faces were generated with points on regular arches on previously specified distances. They will lead the narrowing method. The linear texture was suit on the generated surface adapting to the half parts of the model and the scanned geometry. Ultimately the final surface was generated by narrowing the cylindrical surface on the point cloud using as a reference the points on the previously created arches. Than the extra areas of the surface which extends over the border of the point cloud were cut. Solid model was generated by thickening the surface. In this method we didn't use the inner scan data.

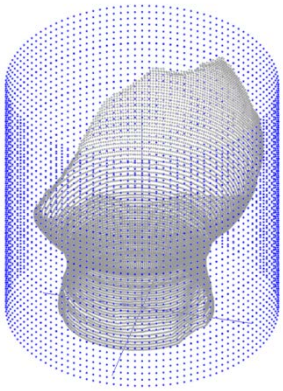

Figure 3. The point cloud and the generated points

Figure 4. Generation of the final surface and the body

All these steps need programming abilities. Homogeneous coordinate transformations were used in the transformation method to find the correct location of the surface point among the scan points in MATLAB.

4. Visualization

To prepare a realistic texture, distortions were needed. This was necessary because the texture was based on the side view of the rotated photographs. In the method we developed, a flat pattern was created with linear matching on the cylindrical surface. Later in the process this cylindrical face will narrow on the previously gained data of the point cloud.

At the first step slices were chopped and distorted in horizontal way from the generated photographs based on the largest diameter of the vase. All of our calculations were based on the pixels of the photographs. The distortion was made on all slices in selected diameters. The lamination was referred to the widest diameter of the vase. Then the slices were merged in panorama maker software in linear merge type. The transparency was set in those places where the cover of the vase was pitted. On those places where the coated areas were missing the original material of the vase was appeared. It was helpful to generate a more realistic visage.

Figure 5. Distortion of the slices and the flat pattern of the texture

To finish our project the original studio settings were reconstructed in the render module of the PTC Creo called Photolux (Figure 6). All the previously measured amounts were recreated and the piece was put in the original place as in the studio. In this environment rendered pictures and videos were made from the solid model. All the settings of the material and the lightings were adjusted until we get the same visage as the originally taken picture.

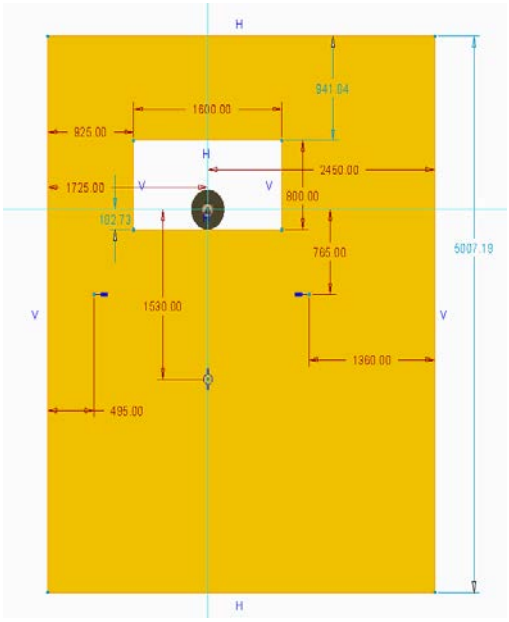

Figure 6. The reconstruction of the photostudio in CAD system

5. Conclusion

Obviously simplifications were made in this representation of our method, but in the future we have plans how to eliminate them to develop the technique for free-form surfaces. It will be useful in industry and medicine as well as restoration.

Figure 7. The original and the rendered picture

As a consequence of the method validations were made relative to the CAD model to substantiate our results on the geometry and the texture mapping. (Figure 7). Verifications were created to certify the relations between the scanned point cloud and the solid geometry as well as the photographs with the rendered pictures.

The usage of the technique is very extensive. The reconstructed pieces can be demonstrated in virtual exhibitions where the user can see the objects placed in original environment beneath a walk through ancient or medieval times.

On the other hand we able to supplement the missing parts to help and simplify the restorations. We can make exact calculations to create the perfect replacement for the piece. Computer aided simulations on the virtual models can be detect the weak and critical parts to avoid the further damages.

(Participants of the project:C3D Ltd., Department of Machine and Product Design - BUTE, Technical University of Dresden, Eötvös Loránd University, University of Óbuda, Department of Polimertechnics - BUTE, Museum of Applied Arts.)

REFERENCES

[1] Montegranario, H.–Espinosa, J.–C.-A. (2007): *A regularization approach for surface reconstructionfrom point clouds*. Applied Mathematics and Computation 188 (2007), ELSEVIER, pp. 583–595.

[2] Liu, S.–Wang, C. C. L. (2010): *Orienting unorganized points for surface reconstruction*. Computers & Graphics 34 (2010), ELSEVIER, pp. 209–218.

[3] Alberts, C. A. (2004): *Surface reconstruction from scan paths*. Future Generation Computer Systems 20 (2004), ELSEVIER, pp. 1285–1298.

[4] Sotoodeh, S.–Gruen, A.–Hanusch, T.: *Integration of structured light and digital camera image data for the 3D reconstruction of an ancient globe.* ISPRS Congress Beijing 2008 conference, Beijing, China, 2008. July 3–11, pp. 367–372.

[5] De Reu, J.–Plets, G.–Verhoeven, G.–Bats, M.–Herremans, D.–Clercq, W. D. (2012): *Towards a three-dimensional cost-effective registration of the archaeological heritage*. Journal of Archaeological Science (2012)

[6] Koutsoudis, A.–Pavlidis, G.–Arnaoutoglou, F.–Tsiafakis, D.–Chamzas, C. (2007): *Qp: A tool for generating 3D models of ancient Greek pottery.* Journal of Archaeological Science (2009)

REVIEWING COMMITTEE

University of Miskolc, Department of Research Management and International Relations
Responsible for publication: Prof. Dr. Tamás Kékesi
Miskolc-Egyetemváros
Published by the Miskolc University Press under leadership of Erzsébet Burmeister
Editor: Dr. Ágnes Takács
Number of copies printed: 49
Put to Press in 2013
Number of permission: TNO – 2013 – 40 – ME HU ISSN 1785-6892